

# Fabrication of High Aspect Ratio Silicon Nanostructure with Sphere Lithography and Metal-Assisted Chemical Etching and Its Wettability

Nobuyuki Moronuki\*, Nguyen Phan\*\*, and Norito Keyaki\*\*\*

\* Tokyo Metropolitan University  
6-6 Asahigaoka, Hino, Tokyo 191-0065, Japan  
E-mail: moronuki@tmu.ac.jp

\*\* Tokyo Metropolitan University  
6-6 Asahigaoka, Hino, Tokyo 191-0065, Japan  
E-mail: phan-nguyenbinh@ed.tmu.ac.jp

\*\*\* Mitsubishi Plastics, Inc  
5-8 Mitsuya, Nagahama, Shiga 526-8660, Japan  
E-mail: keyaki.norito@ma.mpi.co.jp

**Metal-assisted chemical etching (MACE) is site-selective etching process due to catalyst reaction at the interface between noble metal and silicon. This paper aims to make clear the applicability of sphere lithography and MACE to fabricate high aspect ratio Si nanostructures. The capacity to control the etched profiles and scale extension were investigated. Firstly, silica particles (e.g.  $\phi 1 \mu\text{m}$ ) were self-assembled on a Si substrate. After the reduction of particle size by argon ion bombardment, a gold layer was deposited using the particles as a mask. The substrate was then etched with mixture of hydrofluoric acid and hydrogen peroxide. It was found that an array of nanopillars was produced with regular pitch, good separation and aspect ratio reached about 52. Effect of MACE conditions on final profiles was made clear. Limitation of this approach is small range of fabricated area (several millimeters) due to the dependence on vacuum technique (ion bombardment, Au deposition) which limited its practical applications. Thus Ag nanoparticle (e.g.  $\phi 150 \text{ nm}$ ) was applied. Relationship between concentration of Ag suspension, Ag assembled layer and morphology of MACE structures was made clear. Spray method was applied to extend deposited area of Ag particles up to  $\phi 100 \text{ mm}$ . Finally, effect of cross-sectional profile on the contact angle of water droplet was examined. By applying high aspect ratio nanostructure on the substrate, the water contact angle increased up to 153 degrees while that without structure was 58 degrees.**

**Keywords:** metal-assisted chemical etching, sphere lithography, structured surface, high aspect ratio, wettability

## 1. INTRODUCTION

Artificial silicon structured surfaces have attracted increasing attention because of their versatile functions, such as self-cleaning [1, 2], light emitting [3], energy conversion and energy storage [4]. High aspect ratio

nanostructures are often required to enhance the functionality due to their high surface ratio [5]. Numerous processes have been proposed to produce these structures, including Bosch process [6], electrochemical etching [7], vapor-liquid-solid (VLS) growth [8]. However most of the methods are associated with problems, for example complexity, expensive equipments or difficulty in control. Thus a simple, effective and well-controlled fabrication method is necessary.

Metal-assisted chemical etching is site-selective and directional etching of silicon in which noble metal works as a catalyst. To obtain desired structures, patterning of metal layer becomes important. Sphere lithography can be used to make metal pattern directly or indirectly. A monolayer assembly of fine particles on a silicon substrate can play a role of mask. For example, silica particles can be self-assembled in monolayer on a substrate [9]. After the reduction of particle size, gold layer can be deposited using the particles as a mask. As a result, gold layer that has openings with regular pitch can be obtained. After etching in solution of hydrofluoric acid and hydrogen peroxide, ordered arrays of Si nanopillars can be obtained.

Limitation of this approach is small range of fabricated area (several millimeters) due to the dependence on vacuum technique (the reduction step and Au deposition step). It can be solved by using self-assembly of silver particles, metal pattern will be formed directly. Key is regular assembled structure of Ag particles in a wide range. However there were few studies that investigate the variation or controllability of the profile as well as scale extension of fabricated area when using self-assembly of particles and MACE [10-12].

This paper aims to make clear the applicability of particle self-assembly and MACE to fabricate high aspect ratio nanostructures, the controllability and the scale extension capacity. In the latter part, the wettability of the structured surface and effects of structural design will be discussed aiming at self-cleaning surface as the final application.

## 2. FABRICATION PROCESS

### 2.1. Background of Metal-Assisted Chemical Etching

Figure 1 shows a mass transport model of metal-assisted chemical etching using metal thin film for catalyst. Firstly Si atoms at the interface of metal layer and Si substrate are oxidized and porous Si layer is formed. Through this layer, the HF can diffuse to the bulk Si to facilitate the dissolution. Then the reactants and byproducts also diffuse through the porous layer. The overall reaction is:

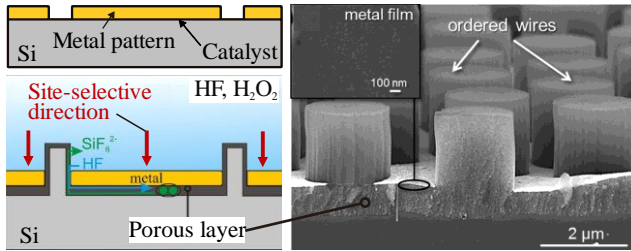
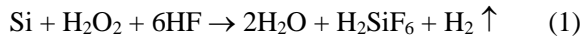


Fig. 1. Mass transport model of MACE [13]

### 2.2. Stiction Phenomenon

Ideally, increasing etching time will produce high aspect ratio structure. However the free-ends of Si nanopillars get together due to the attraction force of rinse solution during the evaporation process, this phenomenon is called stiction. The meniscus force plays an important role not only in this case but also in other fabrication of nanostructure [14, 15].

To minimize stiction, supercritical drying can be used. Using this method, silicon nanopillars with aspect ratio as high as 220 were fabricated [16]. Supercritical drying goes beyond the critical point of the working liquid or the two phase changes in freeze-drying (liquid→solid→gas) in order to avoid the direct liquid-gas transition that will cause attraction between nanopillars. However it is very complicated process. Instead a simple method can be applied by using low surface tension etchant and rinse solution (alcohol) combined with baking to control drying step. Silicon nanopillars with aspect ratio as high as 180 were fabricated without stiction [17].

### 2.3. Fabrication Procedures

Figure 2 shows the schematic of fabrication procedures using (a) silica particle or (b) silver particle. In Fig. 2(a), the procedure started from self-assembly of a monolayer of silica particles on a Si substrate. At this step, dip coating method was applied where the substrate was drawn up from a suspension in which particles were dispersed. Ideally, monolayered hexagonal packed structure can be obtained. Next this layer was dry etched with argon ions to decrease the particle diameter. The dry etching time determines the reduction of the diameter. Then a gold layer was deposited through the particles using electron cyclotron resonance (ECR) sputtering

apparatus. Whereas in Fig. 2(b), silver particles were self-assembled on another Si substrate. Final stages of both are metal-assisted chemical etching. The substrates were etched with a mixture of hydrofluoric acid and hydrogen peroxide. Arrays of silicon nanopillars with regular pitch, high aspect ratio were aimed in this study.

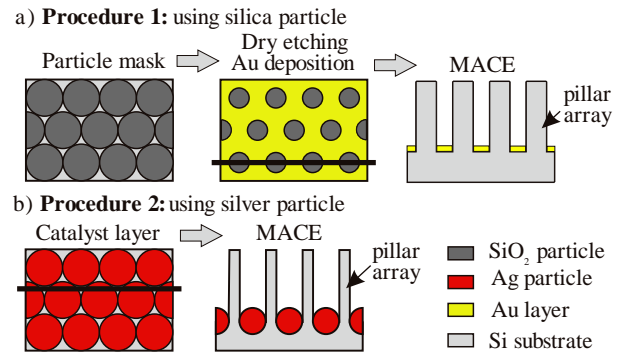


Fig. 2. Fabrication procedures

Table 1 shows the experimental conditions of the process in Fig. 2(a) including the variable parameters. Sodium dodecyl sulfate is a surfactant added to improve dispersity of silica particle in suspension. Here the etchant was diluted by ethanol rather than water to reduce the meniscus force that correlates to stiction between the pillars. In addition, it will help to improve etching rate controllability and stability of Au layer in the etchant. Without the dilution, Au layer was peeled off easily when the substrate was dipped into the etchant.

Table 1. Experimental condition for silica particle

Procedure 1: Fig. 2(a)		
<b>Substrate material/size</b>		
Silicon (100), 10 mm × 10 mm		
<b>Self-assembly</b>	Suspension	Water, silica $\phi$ 1 $\mu\text{m}$ ; 10 wt%, sodium dodecyl sulfate; 0.15 wt%
	Draw up speed/angle	50 – 100 $\mu\text{m/s}$ , 30° – 60°
<b>Dry etching time</b>		
10 min – 15 min		
<b>Au film thickness</b>		
16 nm		
<b>MACE condition</b>	Etchant	HF:H <sub>2</sub> O <sub>2</sub> :Ethanol=3:1:6
	Temperature	20 °C
	Etching time	5, 10, 15, 20 min
<b>Rinse solution</b>		
Ethanol		
<b>Drying condition</b>		
Baking at 60 °C		

## 3. RESULT AND DISCUSSION

### 3.1. Structuring with Procedure 1

Figure 3(a-c) shows scanning electron microscope (SEM) images (top view) of self-assembled silica particles, dry etched particles and Si nanopillar array correspond with 3 steps of the procedure in Fig. 2(a). Assembled particles were hexagonal packed in monolayer. After dry etching step, particle diameter reduced while keeping both the pitch equal to particle

diameter and the hexagonal packed profile. The structure spread over several millimeter range. After MACE step, well-ordered nanopillar structure was obtained. The diameters of pillars corresponded with that of the particles and dry etching conditions. **Fig. 3(d)** shows the relationship between etched depth (height of structure) and etching time. The depth increased with the etching time almost linearly and the etching rate was found to be around  $1.7 \mu\text{m}/\text{min}$ . Structure with aspect ratio as high as 52 without stiction was obtained. Thus with the combination of sphere lithography, dry etching and MACE, the morphology of structures can be well controlled including pillar diameter, pitch and height.

Inset image in **Fig. 3(d)** shows top view of the MACE structure with  $\text{AR} = 68$ . At this height, the stiction phenomenon started to occur. The phenomenon could be observed more clearly when the substrate was etched in high surface tension etchant (ethanol was replaced by water) and fast drying by nitrogen gas. **Fig. 4(a, b)** shows the top view and sectional view of MACE structure respectively, the silicon nanopillars were distorted to form big clustering at their tips when their height was about  $9 \mu\text{m}$  ( $\text{AR} = 18$ ). The mechanism was schematically explained in **Fig. 4(c)**. Therefore combination of low surface tension etchant and controllable drying step is a simple and effective method to obtain high AR nanostructures without stiction.

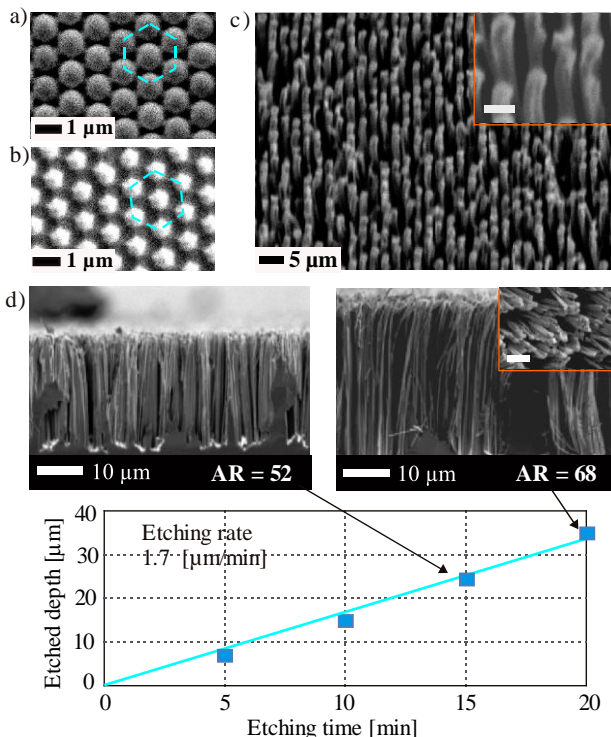


**Fig. 3.** High aspect ratio Si nanostructure: (a) Hexagonal packed monolayer of  $\phi 1 \mu\text{m}$  silica particle, (b) Corresponding dry etched particle layer, (c) Top SEM view of MACE structure, inset scale bar is  $1 \mu\text{m}$ , (d) Relationship between etched depth and etching time, inset scale bar is  $3 \mu\text{m}$ .

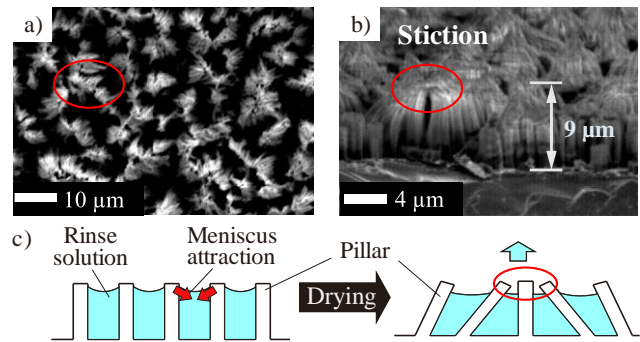


**Fig. 4.** Stiction phenomenon when using high surface tension etchant: (a) Top view and (b) Cross-sectional view of structure, (c) Schematic explanation.

### 3.2. Structuring with Procedure 2

Combination of self-assembly of silica particle and dry etching is an effective method to pattern Au layer that permit to control the profile of nanostructures. However there is the size limitation. Both of dry etching process and Au deposition process need vacuum environment. In addition, high energy dry etching apparatus, used to reduce particle diameter, can focus on small area as centimeter range. These properties limit scale extension ability of the process. Replication and roll imprint might be useful. But aspect ratio is limited because of low strength of plastic materials for replicated product.

Self-assembly of noble metal particles was used to eliminate the dependence on vacuum technique (**Fig. 2(b)**). Firstly dropping method, the simplest deposition method, was used to deposit Ag particles on a silicon substrate. After evaporation of water, aggregated structure remained on the substrate and it was dipped into etchant. This process aims to find the relationship between concentration of Ag suspension, self-assembled Ag structure, and MACE structure before extension of deposited area is done. Experiments when using Ag particles were carried out according to the conditions in **Table 2**. Here the etchant was diluted aiming at the improvement of the etching depth controllability. Average etching rate of the diluted was  $860 \text{ nm}/\text{min}$  while that without dilution was fast as  $10 \mu\text{m}/\text{min}$ .

**Table 2.** Experimental condition for Ag nanoparticle

Procedure 2: Fig. 2(b)		
Self-assembly	Suspension	Water, silver $\phi 150 \text{ nm}$
	Concentration	0.1, 0.2, 0.3, 0.5, 1 wt%
	Drop volume	$50 \mu\text{l}$
MACE condition	Etchant	$\text{HF}:\text{H}_2\text{O}_2:\text{H}_2\text{O}=3:1:12$
	Temperature	$30 \text{ }^\circ\text{C}$
	Etching time	30 min

**Figure 5** shows the observation results of the particle layers and corresponding etched structures with a SEM.

The effect of the concentration of suspension can be seen from the figure. The coverage increased with the concentration. However, it was also found that the particle aggregate size was not constant but varies up to micron level and multi-layered. Lower part of **Fig. 5** shows the cross-sectional observation of the etched structures. High aspect ratio profiles were obtained however the maximum depth decreased with the increase in the concentration. In addition, the etched depth was changed with the lateral position while catalyst reaction with Au film produced almost constant depth (**Fig. 3**). The cause of the depth fluctuation is considered as the difference in the aggregation size as shown in the upper part of **Fig. 5**. The formation of pore or pillar arrays is affected by the coverage of Ag particles and can be explained schematically as in **Fig. 6**. Regular pillar structures can be obtained only when the particles are assembled in pack structure in monolayer. In other conditions, irregular pore or pillar are obtained.

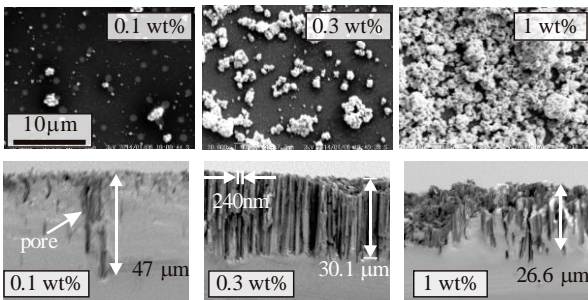


**Fig. 5.** MACE with Ag nanoparticles.

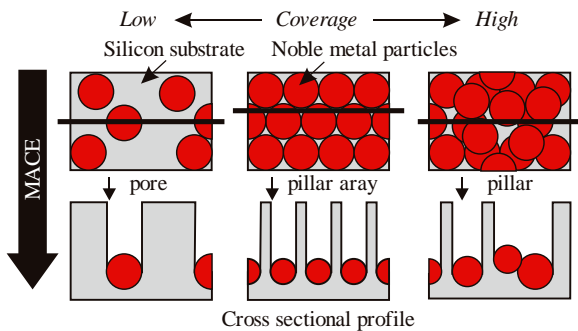


**Fig. 6.** Explanation for pore/pillar formation.

**Figure 7** summarizes the effect of the Ag particle concentration on the coverage calculated by using an image processing software. It was found that the coverage increased linearly with the concentration, which suggests the controllability of coverage by adjusting the concentration.

Properties of MACE with Ag particles was made clear. It was found the uniformities of aggregation size and distribution are crucial to obtain constant pore/pillar diameter, pitch and depth. Next step is scale extension of deposition area that help to extend structuring area.

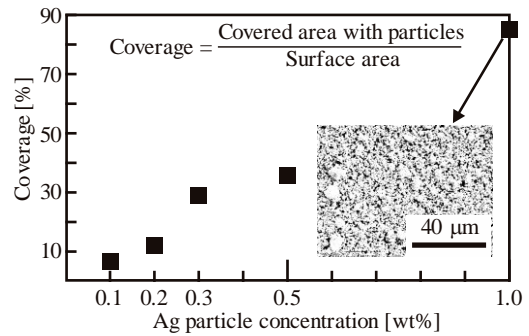


**Fig. 7.** Effect of Ag particle concentration on etched depth.

### 3.3. Extension of the Deposition Area

Former results suggest the controllability of not only pore/pillar concentration but its depth over a wide range. However the structuring area is limited as far as dropping method is applied. To extend of the structuring area, spray method was tried. The schematic of design is shown in **Fig. 8**. Using ultrasonic spray, mist of the Ag suspension was produced and guided onto a silicon substrate that was put on a hot plate to speed up the evaporation of water. Using this apparatus, the structuring area was extended to φ100 mm. However the coverage was limited up to 30% (**Fig. 9**). Further remodeling of the setup is necessary.

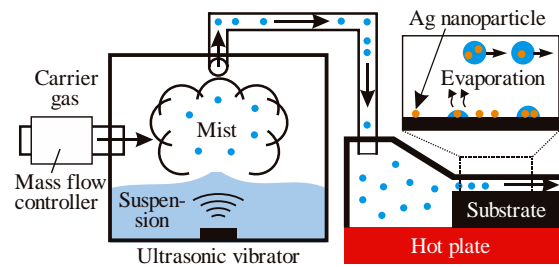


**Fig. 8.** Schematic of spray equipment.

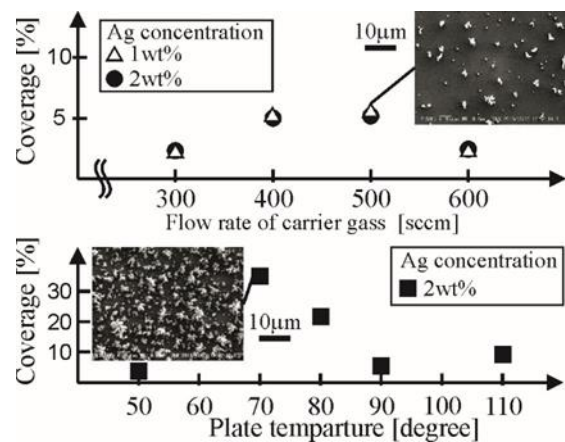


**Fig. 9.** Effect of spray conditions on the coverage of Ag particles.

### 3.4. Control of the Wettability as a Functionality

The wettability of a solid surface can be modified with its structural design (pillar diameter, pitch and aspect ratio) and its surface energy. With suitable parameters, all vacant spaces between the structures can be filled with water and all surface becomes wet (Wenzel state). Otherwise water droplet only lies on the tips of the structures that shows stable air trap under the droplet (Cassie-Baxter state). The transition condition between two states has not been made clear but generally much air trap will lead to high water contact angle [18, 19].

**Figure 10** shows the effect of structural aspect ratio on the contact angle of water droplet. The relationship was not linear. With the increase in aspect ratio, the contact angle increased continuously due to much air was entrapped. Further investigation is necessary. It was also confirmed that hydrophilic silicon surface could be changed to superhydrophobic (water contact angle = 153°).

With similar aspect ratio (around 15), the structure fabricated using silica particles had larger contact angle than the structure fabricated using Ag particles. The reason is considered as imperfect structure when using Ag particles.

The oxide layer of silicon is originally hydrophilic. Water droplets are sticky on the structured surface in spite of having high contact angle. To achieve self-cleaning function, that affords easy movement of water droplets, surface modification may be essential. Fluoresin coating [2, 20-21] or deposition of self-assembled monolayer (SAM) of silanes can be potential additional processes [9, 15, 22-24].

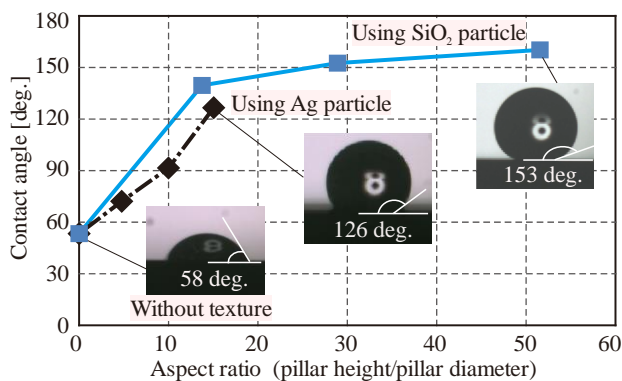


**Fig. 10.** Effect of aspect ratio on contact angle of water droplet.

## 4. CONCLUSION

The nanopillar structures can be produced with good controllability by using self-assembly of silica particles, dry etching and metal-assisted chemical etching. High aspect ratio structure was obtained without stiction of nanopillars. The scale extension of structuring area was considered by using self-assembly of silver particles. Basic properties of metal-assisted chemical etching of silicon with Ag nanoparticle catalyst were made clear.

Various structures with different pattern and depth were obtained by changing the deposition condition. Finally, wettability control was demonstrated and hydrophilic substrate was changed to superhydrophobic one.

The improvement of Ag particle dispersity is one of the future problems to enhance the morphology controllability. Other one is surface modification to obtain durable self-cleaning surfaces.

### Acknowledgements

This work was supported by Asian Human Resources Fund of Tokyo Metropolitan Government.

### REFERENCES:

- [1] T. Liu, and C-J. Kim, "Turning a surface superrepellent even to completely wetting liquids," *Science*, vol. 346, pp. 1096-1100, 2014.
- [2] N. Moronuki, A. Takayama, A. Kaneko, "Design of surface texture for the control of wettability," *Trans. JSME*, vol. 70, pp. 1244-1249, 2004.
- [3] W. Chern, et al, "Nonlithographic Patterning and Metal-Assisted Chemical Etching for Manufacturing of Tunable Light-Emitting Silicon Nanowire Arrays," *Nano Letters*, vol. 10, pp. 1582-1588, 2010.
- [4] K. Q. Peng, et al, "Silicon nanowires for advanced energy conversion and storage," *Nanotoday*, vol. 8, pp. 75-79, 2013.
- [5] N. Moronuki, "Functional texture design and texturing processes," *Int. J. of Automation Technology*, vol. 10, pp. 4-15, 2016.
- [6] S. A. McAuley, H. Ashraf, L. Atabo, A. Chambers, S. Hall, J. Hopkins, G. Nicholls, "Silicon micromachining using a high density plasma source," *J. Phys. D: Appl. Phys.*, vol. 34, pp. 2769-2774, 2001.
- [7] Y. Xiu, S. Zhang, V. Yelundur, A. Rohatgi, D. W. Hess, and C. P. Wong, "Superhydrophobic and low light reflectivity silicon surfaces fabricated by hierarchical etching," *Langmuir*, vol. 24, pp. 10421-10426, 2008.
- [8] Z. Zhang, T. Shimizu, S. Senz, U. Gosele, "Ordered high-density Si [100] nanowires arrays epitaxially grown by bottom imprint method," *Adv. Mater.*, vol. 21, pp. 2824-2828, 2009.
- [9] M. Nishio, N. Moronuki, and M. Abasaki, "Fabrication of patterned Ag and Au inverse opal structures through repeated self-assembly of fine particles," *Int. J. of Automation Technology*, vol. 8, pp. 755-760, 2014.
- [10] Z. Huang, H. Fang, and J. Zhu, "Fabrication of silicon nanowire arrays with controlled diameter, length and density," *Adv. Mater.*, vol. 19, pp. 744-748, 2007.
- [11] K. Peng, M. Zhang, A. Lu, N-B. Wong, R. Zhang, S-T. Lee, "Ordered silicon nanowire arrays via nanosphere lithography and metal induced etching," *App. Phys. Lett.*, vol. 90, pp. 163123-3, 2007
- [12] D. Qi, N. Lu, H. Xu, B. Yang, C. Huang, M. Xu, L. Gao, Z. Wang, L. Chi, "Simple approach to wafer-scale self-cleaning antireflective silicon surfaces," *Langmuir*, vol. 25, pp. 7769-7772, 2009.
- [13] N. Geyer, B. Fuhrmann, Z. Huang, J. Boor, H. S. Leipner, and P. Werner, "Model for mass transport during metal-assisted chemical etching with contiguous metal films as catalyst," *J. Phys. Chem. C*, vol. 116, pp. 13446-13451, 2012.
- [14] N. Hussing, and U. Schubert, "Aerogel – airy material: chemistry, structure, and properties," *Angew. Chem. Int. Ed.*, vol. 37, pp. 22-45, 1998.
- [15] H. Jin, M. Kettunen, A. Laiho, H. Pynnonen, J. Paltakari, A. Marmur, O. Ikkala, and R. H. A. Ras, "Superhydrophobic nanocellulose aerogel membranes as bioinspired cargo carriers on water and oil," *Langmuir*, vol. 27, pp. 1930-1934, 2011.
- [16] S-W. Chang, V. P. Chuang, S. T. Boles, C. A. Ross, and C. V. Thompson, "Densely packed arrays of ultra-high-aspect-ratio silicon nanowires fabricated using block-copolymer lithography and metal-assisted chemical etching," *Adv. Funct. Mater.*, vol. 19, pp. 2495-2500, 2009.

- [17] K. Balasundaram, et al, "Porosity control in metal-assisted chemical etching of degenerately doped silicon nanowires," *Nanotechnology*, vol. 23, pp. 305304-305310, 2012.
- [18] R. N. Wenzel, "Resistance of solid surfaces to wetting by water," *Ind. Eng. Chem.*, vol. 28, pp. 988-994, 1936.
- [19] A. B. D. Cassie, and S. Baxter, "Large contact angles of plant and animal surfaces," *Nature*, vol. 155, pp. 21-22, 1945.
- [20] B. S. Kim, S. Shin, S. J. Shin, K. M. Kim, and H. H. Cho, "Control of superhydrophilicity/superhydrophobicity using silicon nanowires via electroless etching method and fluorine carbon coatings," *Langmuir*, vol. 27, pp. 10148-10156, 2011.
- [21] H. Hu, et al, "Hierachically structured re-entrant microstructures for superhydrophobic surfaces with extremely low hysteresis," *J. Micromech. Microeng.*, vol. 24, pp. 095023-095030, 2014.
- [22] S. R. Wasserman, Y. T. Tao, G. M. Whitesides, "Structure and reactivity of alkylsiloxane monolayers formed by reaction of alkyltrichlorosilanes on silicon substrate," *Langmuir*, vol. 5, pp. 1074-1087, 1989.
- [23] C. Lee, and C. Kim, "Maximizing the giant liquid slip on superhydrophobic microstructures by nanostructuring their sidewalls," *Langmuir*, vol. 25, pp. 12812-12818, 2009.
- [24] A. Kaneko, and I. Takeda, "Textured surface of self-assembled particles as a scaffold for selective cell adhesion and growth," *Int. J. of Automation Technology*, vol. 10, pp. 62-68, 2016.